FLEXIBLE: Forecasting Cellular Traffic by Leveraging Explicit Inductive Graph-Based Learning

Duc-Thinh Ngo*†, Kandaraj Piamrat†, Ons Aouedi‡, Thomas Hassan*, Philippe Raipin*

* Orange Innovation, Cesson-Sévigné, France

† Nantes University, École Centrale Nantes, IMT Atlantique, CNRS, INRIA, LS2N, UMR 6004, Nantes, France

‡ SnT, SIGCOM, University of Luxembourg, Luxembourg

Abstract—From a telecommunication standpoint, the surge in users and services challenges next-generation networks with escalating traffic demands and limited resources. Accurate traffic prediction can offer network operators valuable insights into network conditions and suggest optimal allocation policies. Recently, spatio-temporal forecasting, employing Graph Neural Networks (GNNs), has emerged as a promising method for cellular traffic prediction. However, existing studies, inspired by road traffic forecasting formulations, overlook the dynamic deployment and removal of base stations, requiring the GNN-based forecaster to handle an evolving graph. This work introduces a novel inductive learning scheme and a generalizable GNN-based forecasting model that can process diverse graphs of cellular traffic with one-time training. We also demonstrate that this model can be easily leveraged by transfer learning with minimal effort, making it applicable to different areas. Experimental results show up to 9.8% performance improvement compared to the state-of-the-art, especially in rare-data settings with training data reduced to below 20%.

Index Terms—Network traffic prediction, time series data, spatiotemporal forecasting, graph neural networks, transfer learning

I. INTRODUCTION

Network traffic prediction is crucial for efficient network management, providing operators with insights for optimization. In a zero-touch network, traffic prediction can continuously inform the monitoring components about future network conditions, enabling timely decision-making. Framed as a time-series forecasting problem, predicting network traffic involves identifying the best model using historical data for accurate future predictions. Recently, spatiotemporal forecasting based on Graph Neural Networks (GNNs) has emerged as a promising approach, capturing correlations between traffic patterns of Evolved NodeBs (eNBs). For instance, geographically proximate eNodeBs can exhibit similar traffic volumes due to comparable population densities. Additionally, depending on users' mobility patterns during network usage, network traffic state can be *propagated* from one eNB to another.

Spatiotemporal forecasting typically requires a pre-constructed graph of correlations, often based on eNBs proximity. Existing works [1], [2] conduct spatiotemporal prediction for an entire city in one go, relying on a single proximity graph for the city's network infrastructure. While advantageous for capturing long-range correlations, this approach be-

comes *rigid* - heavily dependent on the input graph. Therefore, any addition or removal of eNBs requires reinitialization and retraining, incurring extra computing costs. Additionally, the limited data from newly deployed eNBs leads to the scarce data scenario for traffic forecasting model training. Hence, transferring the model to a different city poses challenges due to differing network infrastructures. This is also the difference between transductive and inductive graph learning where in the former, the evaluated nodes are known and in the latter, they can include even unseen nodes during training time.

To address these limitations, we propose **FLEXIBLE** - *Forecasting Cellular Traffic by Leveraging Explicit Inductive Graph-Based Learning*. To the best of our knowledge, this is the first inductive GNN-based model for cellular traffic prediction. Focused on forecasting individual eNBs, it extracts local spatial correlation from the k-hop subgraph centered at the target eNB, combining it with temporal information for accurate predictions. Its inductive design allows operation on unseen nodes during training, ensuring adaptability. By reframing the problem to predict individual traffic within its local k-hop graph, FLEXIBLE homogenizes graph topologies and regularizes the spatiotemporal model, enhancing generalizability. This simplifies transfer learning into a direct scheme without additional steps, in contrast to prior methods like [3]–[7]. Despite the limitations of exploiting only local information, FLEXBILE gains the possibility to perform prediction on unseen eNBs and its straightforward transfer learning mechanism. Indeed, by experimental results, we show that when the data for training is very few, a pre-trained FLEXIBLE that is finetuned on a new city's traffic data can outperform state-of-the-art models.

II. RELATED WORKS

A. Graph Neural Networks - GNNs

GNNs are widely recognized in the deep learning literature for their ability to handle irregular data, specifically graphs. Early research focused on formulating convolutional operators for graphs, with Fast spectral filtering [8] being a pioneering work that implemented convolution in the spectral space of graphs. Subsequent works further simplified the computation

TABLE I
Table of notation

Notation	Description
$\boldsymbol{X}_i^{(t)}$	Traffic value of i-th node at t-th timestep
dist(i, j)	Geographical distance between locations of i and j
T_h	Number of historical steps
T_f	Number of prediction steps
$\mathcal{T}$	Set of timesteps
$\mathcal{V}$	Set of eNBs
$\boldsymbol{x}_{i,t}$	$\boldsymbol{X}_i^{(t-T_h:t)}$
$\boldsymbol{y}_{i,t}$	$\boldsymbol{X}_i^{(t:t+T_f)}$
$\boldsymbol{h}_i^{(l)}$	Hidden features of node i extracted at the l-th layer
p	Edge dropout probability
d	Dilation factor within the dilated convolution operator
C	Number of hidden features
L	Number of spatiotemporal blocks
λ	Weight decay
$\mathcal{K}$	Set of kernel sizes
B	Batch size

by representing the convolutional operator as a stack of 1-hop filters [9]. This approach, often referred to as Message-Passing Neural Network (MPNN), relies on two differentiable functions: message aggregation within a local neighborhood and node updates based on the aggregated message. In the context of spatiotemporal graphs with node features containing temporal data, leveraging GNN insights becomes crucial for developing models adept at capturing graph dynamics.

B. Spatiotemporal forecasting

Spatiotemporal forecasting is an emerging approach to tackle cellular traffic prediction with high precision [1], [2], [7] and it is inspired from the road traffic forecasting [10]–[12]. While extensively researched, existing methods typically address the problem in a transductive setting where the given graph remains constant during both the training and inference phases. This work proposes a more flexible model designed to operate natively in an inductive setting, accommodating scenarios where the graphs differ between the training and inference phases.

C. Transfer learning

In the domain of spatiotemporal prediction, transfer learning across different cities has been extensively explored, particularly when data is scarce. Existing works managed to find workaround solutions to handle the discrepancy between graph topologies in source and target cities. Some approaches, like graph partitioning with padding [3], [4], node2vec-based feature creation [5], clustering algorithms with inter-city region mapping [7], and the transferable mechanism for graph structure learning [6] introduce additional computing costs. The most significant drawback, however, is that all these methods necessitate re-training if the target spatial graph changes.

III. METHODOLOGY

A. Problem definition

The traffic prediction problem is defined as finding an optimal forecasting function f that predicts the future T_f timesteps given the historical T_h timesteps. We denote the multivariate time series representing the entire traffic dataset as $\boldsymbol{X}$ and $\boldsymbol{X}_i^{(t)}$ as a scalar value indicating the traffic of the i-th variable at timestep t. The traffic prediction problem is defined as:

$$\arg\min_f \sum_{t\in\mathcal{T}, i\in\mathcal{V}} \mathcal{L}\left(f\left(\boldsymbol{X}_i^{(t-T_h:t)}\right), \boldsymbol{X}_i^{(t:t+T_f)}\right), \quad (1)$$

where $\mathcal{L}$ is the loss function, $\mathcal{T}$ is the discrete temporal interval, and $\mathcal{V}$ is the set of vertices - in this case - a set of eNBs. Furthermore, we provide all repeatedly used notations in this paper in the Table I.

In contrast to previous studies that adopt transductive settings, splitting only $\mathcal{T}$, we introduce FLEXIBLE. This fully inductive GNN-based model addresses the continuous deployment of eNodeBs, allowing variations in both $\mathcal{T}$ and $\mathcal{V}$ during different phases. To achieve this, we reframe the problem as a graph-level task instead of node-level. For predicting traffic at base station i during the interval $[t, t+T_f)$, we extract the k-hop subgraph centered at node i. This subgraph, along with its nodes' traffic states, is fed into a learned spatiotemporal model for forecasting, represented by:

$$\hat{\boldsymbol{y}}_{i,t} = f(\boldsymbol{A}_k(i), \{\boldsymbol{x}_{j,t} \mid j \in \mathcal{V}_k(i)\}), \quad (2)$$

where $\boldsymbol{A}_k(i)$ is the adjacency matrix of the induced k-hop subgraph around the node i, $\mathcal{V}_k(i)$ is set of nodes involved in the subgraph, and f is the parameterized model. We visualize our pipeline in Figure 1 and describe components in the following sections.

B. Graph construction

1) Proximity graph: Since mobile users are often in movement, we can assume that the nearby eNBs' traffic is correlated. Therefore, we craft a graph of correlation solely based on the geographical position of eNBs:

$$W_{ij}^s = \begin{cases} \exp\left(-\text{dist}(i,j)\right), & \text{if dist}(i,j) < \kappa \text{ and } i \neq j. \\ 0, & \text{otherwise.} \end{cases} \quad (3)$$

where $\text{dist}(i,j)$ is the geographical distance between two eNBs i and j. In both the Paris and Lyon datasets, we set $\kappa = 3.5\text{km}$, which is the minimum distance so that both graphs remain connected. Furthermore, we sparsify the graph by limiting the maximum node degree to 10.

2) k-hop subgraphs: For each node i, we pre-build its k-hop subgraphs from the constructed large proximity graph and store them in a key-value database. Given a pair (i, t), we can efficiently retrieve the subgraph $\boldsymbol{A}_k(i)$ from the database. Additionally, we can access the set of traffic information linked to its vertices at time t using stored node IDs associated with the subgraph. During training, we introduce Edge Dropout to these subgraphs with a probability of p to augment data and mitigate overfitting.

C. Spatiotemporal module

1) Temporal Convolutional Network: In studying time series data, different methods like Convolutional Neural Networks (CNNs), Recurrent Neural Networks (RNNs), and
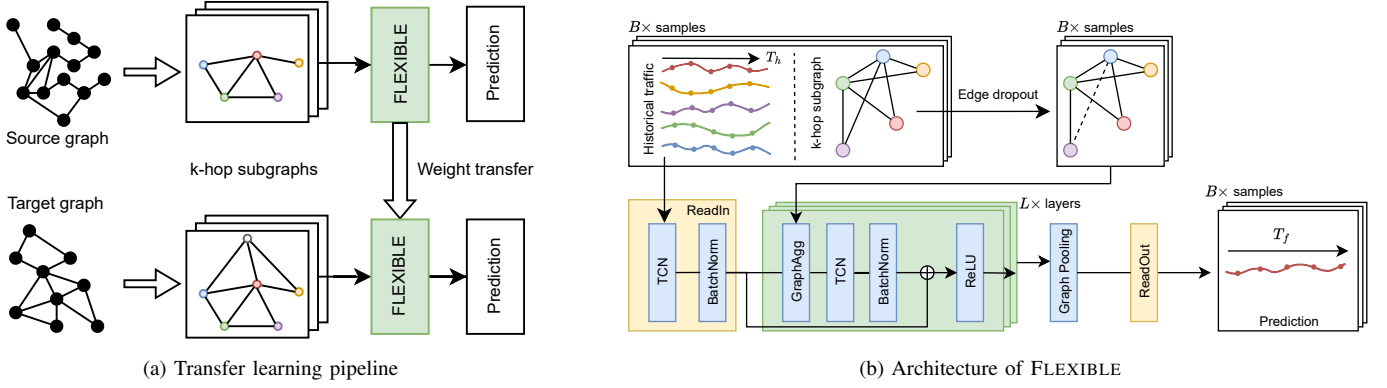
Fig. 1. The proposed frameworks: (a) transferring FLEXBILE from source to target city and (b) model architecture which takes a batch of k-hop subgraphs and associated historical traffic to generate a batch of prediction for the target eNB.

Attention mechanisms are used. Among all of them, the CNN, which is natively designed for parallel computing and requires fewer parameters, is a fast and effective choice for analyzing time series data with good accuracy [10]–[12]. For our approach, a key technique is using dilated causal convolution [13]. This helps capture a broad range of information quickly while maintaining the causality in the features we extract. Furthermore, we follow the Inception-like [14] architecture by having multiple kernel sizes in each dilated causal convolution layer to capture features at multiple scales and rapidly enlarge the receptive field. Given $h \in \mathbb{R}^{T_h \times C}$ as the hidden features of an arbitrary node, the proposed Temporal Convolutional Network (TCN) can thus be described as below:

$$\text{TCN}(h) = \bigcup_{K \in \mathcal{K}}^{\text{concat}} h *_{\text{dc}} f_K \qquad (4)$$

where f_K is the filter of kernel size K and the resulting feature from TCN is the concatenation of all filtered signals corresponding to every kernel size in the set $\mathcal{K}$. Moreover, $*_{\text{dc}}$ is the dilated causal convolution as described in [13] with the dilation exponentially scaled by a factor d after each layer.

2) Graph Isomorphism Network: It has been demonstrated that GNNs can encounter challenges in distinguishing between different graphs in specific cases [15], making them less powerful than the Weisfeiler-Lehman (WL) graph isomorphism test. Addressing this limitation, Xu *et al.* [15] introduced Graph Isomorphism Network (GIN), which has been shown to possess the same discriminative power as the WL test. In the context of our forecasting problem formulated as a graph-level task, the model's ability to capture various graph topologies becomes crucial. Being able to distinguish between different graphs is essential for enhancing the model's expressive power.

Consequently, we inspire from GIN to propose our spatio-temporal model:

$$\text{GraphAgg}(h_i) = (1 + \epsilon) h_i + \sum_{u \in \mathcal{N}(u)} h_u \qquad (5)$$

$$h_i^{(l+1)} = \text{ReLU}\left(\text{TCN}(\text{GraphAgg}(h_i^{(l)})) + h_i^{(l)}\right) \qquad (6)$$

where $h_i^{(l)} \in \mathbb{R}^{T_h \times C}$ is the hidden features of an arbitrary node i extracted from the l-th layer of the model and ϵ is a learned scalar. It has been shown in [15] that the local aggregation in Equation 5 and the TCN followed by ReLU as an approximator are essential elements to build a GNN as powerful as the WL test. Additionally, this design allows the model to be *flexible* so that it can process any graph topology. During transfer learning, only the scalar ϵ and TCN weights are transferred, being independent of graph shapes. To prevent over-smoothing, a residual connection is included, and for practical regularization, batch normalization [16] is applied after each TCN, as illustrated in Figure 1.

D. ReadIn and ReadOut

1) ReadIn: Given the historical traffic $x_{i,t} \in \mathbb{R}^{N \times T_h}$, we process it through a TCN block followed by a batch normalization layer. The extracted features are further processed through a stack of L spatiotemporal layers, as described above.

2) Graph Pooling: The final hidden features are obtained after processing the L-th spatiotemporal layer, resulting in $H \in \mathbb{R}^{N \times T_h \times C}$ corresponding to hidden features of N nodes in the k-hop subgraph. We then apply a graph pooling layer to pool out the final representation that should be used for the prediction. Since we only need to predict the traffic on one target node, we take out only its associated hidden features and call that TargetPooling. We also let a hyperparameter sweep to choose among this and three other poolings considered in [15]: global sum, max, and mean pooling.

3) ReadOut: After Graph Pooling, we acquire a hidden feature $h \in \mathbb{R}^{T_h \times C}$. To produce the prediction, we propose a two-step ReadOut module:

$$\hat{h}[\tau, :] = \text{ReLU}\left(\sum_{l=t-T_h}^{t-1} w_{l\tau} h[l, :] + a_\tau\right) \qquad (7)$$

$$\hat{y}[\tau] = \sum_{c=0}^{C-1} z_c \hat{h}[\tau, c] + b_\tau \qquad (8)$$

where $w_{l\tau}, a_\tau, z_c,$ and b_τ are learnable weights.

E. Loss function

We train the model to minimize the Mean Absolute Arror (MAE) between the prediction and the ground truth while adding a regularization on the norm of the model's parameters to prevent overfitting:

$$\mathcal{L} = \frac{1}{|T_f||\mathcal{T} \times \mathcal{V}|} \sum_{(i,t) \in \mathcal{T} \times \mathcal{V}} \left| \boldsymbol{y}_{i,t} - \hat{\boldsymbol{y}}_{i,t} \right| + \lambda \|\boldsymbol{\Theta}\| \quad (9)$$

where $\boldsymbol{\Theta}$ is the model's learnable parameters and λ is the regularization weight.

IV. EVALUATION

A. Dataset

To evaluate the performance of FLEXIBLE, we utilize the NetMob dataset [17] which covers 77 days of the traffic demand, from March 16, 2019, to May 31, 2019, generated by 68 mobile services across 20 metropolitan areas in France. This is so far the largest and the most recent cellular traffic dataset that we have found. For our experiments, we aggregate the downlink traffic of 5 prominent services in Paris and Lyon: Apple Video, Fortnite, Netflix, Instagram, and Microsoft Mail. These applications were chosen as they collectively represent the majority of cellular traffic. Moreover, they offer a diverse range of content consumption types, aligned with the Quality of Service Class Identifier [18]. By examining the aggregated traffic of these 5 distinct applications, we can benchmark the model's capability to handle complex traffic dynamics.

However, the provided data is the traffic per $100 \times 100 m^2$ tile which is aggregated from several eNBs' traffic based on distance. This format deviates from the real-world scenario where data is typically collected and aggregated per eNB, which is essential for forecasting traffic and performing radio resource management. To address this issue, we combine the spatiotemporal data with the eNB map [19] and use Voronoi tessellation to re-aggregate the traffic into per-eNB traffic:

$$\text{Vor}(i) = \{\text{tile}_m \mid \text{dist}(\text{tile}_m, i) < \text{dist}(\text{tile}_m, j) \forall j \in \mathcal{V}\} \quad (10)$$

$$\boldsymbol{X}_i^{(t)} = \sum_{m \in \text{Vor}(i)} \boldsymbol{T}_m^{(t)} \quad (11)$$

where $\boldsymbol{T}_m^{(t)}$ is the raw traffic of the m-th tile at time t and $\text{Vor}(i)$ is the Voronoi partition of the i-th eNB. Finally, we obtain 1555 and 1230 eNBs for Paris and Lyon respectively, and 7392 timesteps for each as the data resolution is 1 sample per 15 minutes.

B. Experimental settings

1) Overview: Our model is initially trained on Paris traffic in an inductive setting, serving as a pre-trained model for subsequent transfer to the Lyon dataset. Hyperparameter tuning is carried out during this phase. For fine-tuning Lyon traffic, we adopt a transductive setting to facilitate comparisons with state-of-the-art models. In any setting, data is split into three parts: train, validation, and test sets. Training occurs on the train set, with model selection and hyperparameter tuning based on validation set results. Reported results for comparison

TABLE II
Hyperparameters' search space and their optimal values [20].

Hyperparameters	Search space	Optimal value
Learning rate	0.001, 0.003, 0.005, ..., 0.019	0.009
p	0, 0.05, 0.1, 0.15, 0.2	0.05
d	1, 2, 3	1
C	32, 64, 128, 256	64
L	1, 2, 3, 4, 5	2
λ	$10^{-4}, 10^{-5}, 10^{-6}, 10^{-7}$	10^{-5}
$\mathcal{K}$	$\{1, 3\}, \{3\}, \{1, 3, 5, 7\}$	$\{1, 3\}$
B	$\{256, 512, 1024, 2048, 4096\}$	4096
Graph Pooling	Mean, Max, Sum, Target	Target

come from inference on the test set, following the common setting $T_h = 12, T_f = 3$, which are equivalent to 3 hours and 45 minutes respectively.

2) Data split: As elaborated in Section III-A, every data sample can be retrieved via $(i, t) \in \mathcal{T} \times \mathcal{V}$. Accordingly, we split the data by splitting the set $\mathcal{T} \times \mathcal{V}$. We ensure that $|\mathcal{T}_{\text{train}}| = 0.7|\mathcal{T}|, |\mathcal{T}_{\text{val}}| = 0.1|\mathcal{T}|$, and $|\mathcal{T}_{\text{test}}| = 0.2|\mathcal{T}|$. The same factors go for $\mathcal{V}$ splitting. Consequently, the 3 data splits in the inductive setting are $\mathcal{T}_{\text{train}} \times \mathcal{V}_{\text{train}}, \mathcal{T}_{\text{val}} \times \mathcal{V}_{\text{val}}$, and $\mathcal{T}_{\text{test}} \times \mathcal{V}_{\text{test}}$. In a transductive setting, $\mathcal{V}_{\text{train}} = \mathcal{V}_{\text{val}} = \mathcal{V}_{\text{test}} = \mathcal{V}$.

3) Evaluation metrics: We adopt two common metrics to evaluate the models' performance. Given the prediction horizon h, the metrics at each horizon are defined as:

- Root Mean Square Error (RMSE):

$$\text{RMSE}_h = \sqrt{\frac{1}{|\mathcal{T}_{\text{test}}||\mathcal{V}_{\text{test}}|} \sum_{i,t} (\boldsymbol{y}_{i,t}[h] - \hat{\boldsymbol{y}}_{i,t}[h])^2} \quad (12)$$

- Mean Absolute Arror (MAE):

$$\text{MAE}_h = \frac{1}{|\mathcal{T}_{\text{test}}||\mathcal{V}_{\text{test}}|} \sum_{i,t} \left| \boldsymbol{y}_{i,t}[h] - \hat{\boldsymbol{y}}_{i,t}[h] \right| \quad (13)$$

C. Hyperparameter tuning

To tune model hyperparameters effectively, we use Optuna [20], a hyperparameter search framework. We employ default settings for the optimizer, utilizing the Tree-structured Parzen Estimator algorithm [21] for continual downsampling of the search space. Additionally, the median stopping rule is applied for early pruning of less promising trials. The search space and final hyperparameter values are summarized in Table II.

D. Baselines

1) Univariate models:

- **LSTM** [22] is a sophisticated neural network architecture meticulously crafted for the nuanced task of capturing and retaining information within long sequential data.
- **TCN** is a variant of FLEXIBLE, where all graph-related components are removed from the architecture.

2) Multivariate models:

- **DCRNN** [10] is a spatiotemporal model, which leverages dual directional diffusion convolution to capture spatial

Metrics	Horizon	LSTM	TCN	FLEXIBLE
MAE	15 min	2.70 ± 0.004	2.71 ± 0.007	**2.62** ± 0.003
	30 min	3.19 ± 0.002	3.21 ± 0.005	**3.04** ± 0.002
	45 min	3.55 ± 0.004	3.56 ± 0.011	**3.34** ± 0.012
RMSE	15 min	4.53 ± 0.016	4.54 ± 0.019	**4.42** ± 0.021
	30 min	5.26 ± 0.023	5.26 ± 0.010	**5.05** ± 0.021
	45 min	5.64 ± 0.026	5.63 ± 0.008	**5.35** ± 0.005

Metrics	MAE			RMSE		
Horizon (min)	15	30	45	15	30	45
AGCRN	5.04	5.63	6.05	9.73	10.69	11.31
DCRNN	<u>4.84</u>	<u>5.38</u>	<u>5.66</u>	<u>9.34</u>	<u>10.34</u>	<u>10.80</u>
MTGNN	**4.74**	**5.19**	**5.45**	**9.19**	**10.15**	**10.62**
FLEXIBLE	5.13	5.97	6.47	9.84	10.92	11.72
TR-FLEXIBLE	4.98	5.81	6.36	9.41	10.51	11.41

dependencies and incorporates it into a sequence of Gated Recurrent Units to further exploit the temporal dimension.

- **AGCRN** [11] integrates adaptive graph convolutional networks within a sequence of Gated Recurrent Units (GRUs) to capture both node-specific spatial and temporal correlations in traffic series.
- **MTGNN** [12] incorporates self-adaptive graph convolution with mix-hop propagation layers for spatial modules and dilated inception layers for temporal modules.

E. Results of inductive learning

This experiment simulates a real-world scenario where a model trained on traffic data of existing eNBs is used to predict traffic on unseen eNBs. Since multivariate baselines are not natively adapted to inductive settings, in this experiment, we only compare our method with univariate models. Conducted on Paris cellular traffic data, the results in Table III showcase FLEXIBLE outperforming other models across all prediction horizons and evaluation metrics. This underscores the advantage of leveraging spatial correlation and FLEXIBLE's ability to handle graph topology discrepancy between training and inference. Moreover, the comparable performance between LSTM and TCN indicates TCN's effectiveness in capturing sequential information akin to LSTM.

F. Results of transductive learning with full data

To evaluate the effectiveness of our approach relative to multivariate models, we conduct experiments in transductive settings as outlined in Section IV-B. Additionally, we leverage the inductive capability of FLEXIBLE for transfer learning across cities. In this specific trial, we explore traffic data in Lyon, concurrently fine-tuning the FLEXIBLE model previously trained on Paris data to enhance its forecasting performance on Lyon data. We call the transferred model TR-FLEXIBLE.

The results of each model when they are trained or finetuned on 100% of the data, which is 66 days of traffic, are summarized in Table IV. In this setting, MTGNN stays coherent with its claim to outperform other existing methods. Our model, FLEXBILE, due to its *local* nature, cannot achieve prediction as precise as state-of-the-art models. It also highlights that transfer learning does improve the forecasting precision, enabling TR-FLEXIBLE to perform comparably to AGCRN, even better at RMSE-15min and RMSE-30min. However, we believe that these shortcomings become minor when training data is fewer, allowing TR-FLEXBILE to be a better alternative to *global* models when forecasting newly deployed eNBs. In the next section, we present the quantitative results of the data scarcity scenario and demonstrate the performance improvement of FLEXIBLE when data is reduced to below 20%.

G. Results of data-scarcity setting

To assess the forecasting capabilities of newly deployed eNBs, we systematically reduce the volume of training-validation data, investigating the impact on model performance under varying levels of data scarcity: 5%, 10%, 20%, and 40%. In essence, we maintain the test set $\mathcal{T}_{\text{test}}$ unchanged to ensure fair evaluation while progressively dropping the oldest time steps in the training data. This approach ensures that the models are consistently trained with the most recent data, allowing for a comprehensive analysis of their adaptability to limited training information. The validation split is included in this training-validation set and its proportion to the training split is maintained at 1/7. The results are reported in Table V.

We observe that the performance of all models degrades as training data becomes more limited. While, at 40% of data, the performance gaps between models do not change significantly compared to the full data setting. However starting from 20% down to 5%, TR-FLEXIBLE takes the lead in terms of prediction precision. Notably, in the 10% and 20% scenarios, FLEXIBLE, trained exclusively on the target dataset, also outperforms baseline models. This could be due to the *global* models struggling to capture neither temporal nor spatial long-range dependency with limited training data. Moreover, with the complicated design and numerous parameters, the baselines are easily overfitted when the training data is scarce. In contrast, our model, with a compact size and a focus on short-range dependencies, proves more suitable for such situations. We also illustrate the variation of MAE-15min of all models for the amount of training data in Figure 2. Overall, these results highlight the robustness of our model in scenarios with limited data, suitable for traffic prediction of new eNBs and knowledge transfer between cities.

V. CONCLUSION

In this paper, we propose FLEXIBLE, a novel inductive graph-based model for cellular traffic forecasting. We first formulate the problem and describe in detail the dataset we are working on and the technical details of the proposed

TABLE V
MAE of each model in few-shot learning on the cellular traffic in Lyon ($\times 10^5$).

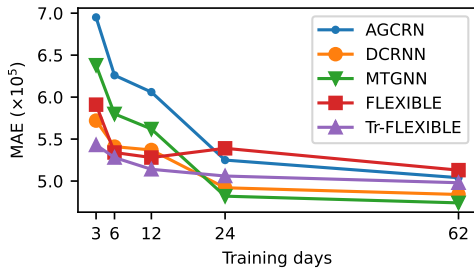| Scarcity rate	5% (~3 days)			10% (~6 days)			20% (~12 days)			40% (~24 days)			Number of
Horizon (min)	15	30	45	15	30	45	15	30	45	15	30	45	parameters
AGCRN	6.95	8.24	9.14	6.26	7.50	8.34	6.06	7.24	8.20	5.25	5.93	6.45	1514715
DCRNN	<u>5.72</u>	6.67	<u>7.36</u>	5.41	6.61	7.56	5.37	6.54	7.35	<u>4.92</u>	<u>5.55</u>	<u>5.96</u>	372353
MTGNN	6.38	7.47	8.44	5.80	6.96	8.25	5.62	6.62	7.75	**4.82**	**5.33**	**5.65**	1861043
FLEXIBLE	5.91	<u>6.61</u>	7.50	<u>5.34</u>	<u>6.30</u>	<u>7.37</u>	<u>5.28</u>	<u>6.10</u>	<u>6.82</u>	5.39	6.16	6.81	140970
Tr-FLEXIBLE	**5.43**	**6.10**	**6.64**	**5.28**	**6.20**	**7.03**	**5.14**	**5.99**	**6.67**	5.06	5.92	6.49	140970

Fig. 2. The MAE at 15min-horizon for the amount of data used for training.

model. Finally, we conduct experiments in 3 settings: inductive learning on Paris data, transfer learning with full data in Lyon, and transfer learning with few data in Lyon. The experimental results prove the capability of learning in inductive and demonstrate the power of FLEXBILE in data-scarcity situations, suggesting it as an alternative model for newly deployed eNBs. Future research should focus on enhancing the model's expressivity for improved prediction accuracy and exploring continual learning techniques for evolving eNB deployment scenarios.

ACKNOWLEDGEMENT

REFERENCES

[1] Y. Fang, S. Ergut, and P. Patras, "SDGNet: A Handover-Aware Spatiotemporal Graph Neural Network for Mobile Traffic Forecasting," *IEEE Communications Letters*, vol. 26, no. 3, pp. 582–586, Mar. 2022.

[2] Z. Wang, J. Hu, G. Min, Z. Zhao, Z. Chang, and Z. Wang, "Spatial-Temporal Cellular Traffic Prediction for 5 G and Beyond: A Graph Neural Networks-Based Approach," *IEEE Transactions on Industrial Informatics*, pp. 1–10, 2022.

[3] T. Mallick, P. Balaprakash, E. Rask, and J. Macfarlane, "Transfer learning with graph neural networks for short-term highway traffic forecasting," in *2020 25th International Conference on Pattern Recognition (ICPR)*. IEEE, 2021, pp. 10 367–10 374.

[4] Y. Huang, X. Song, S. Zhang, and J. J. Yu, "Transfer Learning in Traffic Prediction with Graph Neural Networks," in *2021 IEEE International Intelligent Transportation Systems Conference (ITSC)*. IEEE, Sep. 2021, pp. 3732–3737.

[5] Y. Tang, A. Qu, A. H. Chow, W. H. Lam, S. Wong, and W. Ma, "Domain adversarial spatial-temporal network: A transferable framework for short-term traffic forecasting across cities," in *Proceedings of the 31st ACM International Conference on Information & Knowledge Management*, 2022, pp. 1905–1915.

[6] Y. Jin, K. Chen, and Q. Yang, "Transferable Graph Structure Learning for Graph-based Traffic Forecasting Across Cities," in *Proceedings of the 29th ACM SIGKDD Conference on Knowledge Discovery and Data Mining*. ACM, Aug. 2023, pp. 1032–1043.

[7] Q. Wu, K. He, X. Chen, S. Yu, and J. Zhang, "Deep Transfer Learning Across Cities for Mobile Traffic Prediction," *IEEE/ACM Transactions on Networking*, vol. 30, no. 3, pp. 1255–1267, Jun. 2022.

[8] M. Defferrard, X. Bresson, and P. Vandergheynst, "Convolutional neural networks on graphs with fast localized spectral filtering," in *Advances in Neural Information Processing Systems*, 2016.

[9] J. Gilmer, S. S. Schoenholz, P. F. Riley, O. Vinyals, and G. E. Dahl, "Neural message passing for quantum chemistry," in *Proceedings of the 34th International Conference on Machine Learning - Volume 70*, ser. ICML'17. JMLR.org, 2017, p. 1263–1272.

[10] Y. Li, R. Yu, C. Shahabi, and Y. Liu, "Diffusion convolutional recurrent neural network: Data-driven traffic forecasting," in *International Conference on Learning Representations (ICLR '18)*, 2018.

[11] L. Bai, L. Yao, C. Li, X. Wang, and C. Wang, "Adaptive graph convolutional recurrent network for traffic forecasting," *Advances in neural information processing systems*, vol. 33, pp. 17 804–17 815, 2020.

[12] Z. Wu, S. Pan, G. Long, J. Jiang, X. Chang, and C. Zhang, "Connecting the dots: Multivariate time series forecasting with graph neural networks," in *Proceedings of the 26th ACM SIGKDD international conference on knowledge discovery & data mining*, 2020, pp. 753–763.

[13] A. van den Oord, S. Dieleman, H. Zen, K. Simonyan, O. Vinyals, A. Graves, N. Kalchbrenner, A. W. Senior, and K. Kavukcuoglu, "Wavenet: A generative model for raw audio," *CoRR*, vol. abs/1609.03499, 2016.

[14] C. Szegedy, W. Liu, Y. Jia, P. Sermanet, S. Reed, D. Anguelov, D. Erhan, V. Vanhoucke, and A. Rabinovich, "Going deeper with convolutions," in *2015 IEEE Conference on Computer Vision and Pattern Recognition (CVPR)*, 2015, pp. 1–9.

[15] K. Xu, W. Hu, J. Leskovec, and S. Jegelka, "How powerful are graph neural networks?" in *International Conference on Learning Representations*, 2019.

[16] S. Ioffe and C. Szegedy, "Batch normalization: accelerating deep network training by reducing internal covariate shift," in *Proceedings of the 32nd International Conference on International Conference on Machine Learning - Volume 37*, ser. ICML'15. JMLR.org, 2015, p. 448–456.

[17] O. E. Martínez-Durive, S. Mishra, C. Ziemlicki, S. Rubrichi, Z. Smoreda, and M. Fiore, "The netmob23 dataset: A high-resolution multi-region service-level mobile data traffic cartography," *CoRR*, vol. abs/2305.06933, 2023.

[18] "3GPP TS 23.203 Policy and Charging Control Architecture V17.2.0," Dec. 2021.

[19] T. N. F. Agency, "Cartoradio: The map of radio sites and wave measurements."

[20] T. Akiba, S. Sano, T. Yanase, T. Ohta, and M. Koyama, "Optuna: A next-generation hyperparameter optimization framework," in *Proceedings of the 25th ACM SIGKDD International Conference on Knowledge Discovery and Data Mining*, 2019.

[21] J. Bergstra, R. Bardenet, Y. Bengio, and B. Kégl, "Algorithms for hyperparameter optimization," in *Advances in Neural Information Processing Systems*, J. Shawe-Taylor, R. Zemel, P. Bartlett, F. Pereira, and K. Weinberger, Eds., vol. 24. Curran Associates, Inc., 2011.

[22] S. Hochreiter and J. Schmidhuber, "Long short-term memory," *Neural Comput.*, vol. 9, no. 8, p. 1735–1780, nov 1997.